Morphology of GaAs-quantum-well interfaces grown by liquid-phase epitaxy

U. Morlock
*Max-Planck-Institut für Festkörperforschung, Heisenbergstrasse 1, 7000 Stuttgart 80, Germany**
and Institut für Festkörperphysik I, Technische Universität Berlin, Hardenbergstrasse 36, 1000 Berlin 12, Germany

J. Christen and D. Bimberg
Institut für Festkörperphysik I, Technische Universität Berlin, Hardenbergstrasse 36, 1000 Berlin 12, Germany

E. Bauser and H.-J. Queisser
Max-Planck-Institut für Festkörperforschung, Heisenbergstrasse 1, 7000 Stuttgart 80, Germany

A. Ourmazd
AT&T Bell Laboratories, Holmdel, New Jersey 07733
(Received 13 March 1991)

A quasicolumnar structure of GaAs quantum wells with mean column diameters of $d=1-10$ μm is observed in narrow $Al_{0.4}Ga_{0.6}As/GaAs$ quantum wells prepared by liquid-phase epitaxy. The heterostructures are grown from a Ga solution at $T\approx 650$ °C in a slider boat. Chemical lattice images confirm the presence of narrow quantum wells. The well width, however, can vary by one to two atomic layers over distances of order 9–16 nm. Photoluminescence measurements at $T=2$ K reveal a multiplet of lines for the excitonic $[X(e\text{-hh})_{n=1}]$ transition originating from different columns within each of which the mean well width averaged over the exciton diameter changes by much less than a step height (2.8 Å). The luminescence measurements show that the thickness L_z of the quantum wells varies between 2 and 6 monolayers, with microscopic roughness causing local thickness variations appreciably smaller than one monolayer. Line-shape analysis of the luminescence spectra quantifies the interfacial roughness in terms of a standard deviation $\sigma_{Lz}=0.2-0.4$ monolayer. Time-resolved photoluminescence measurements reveal the same luminescence lifetime of $\tau\approx 270$ ps at $T=4$ K for all spectral lines, with direct or indirect excitation of the quantum well. No significant carrier transfer is observed between the different columns. Cathodoluminescence is used to image the micrometer-scale variations in the quantum-well morphology.

I. INTRODUCTION

Interfaces between adjacent semiconductors, each with different chemical composition and physical properties, are essential constituents of microstructured devices, and provide well-defined samples for basic research.[1] A fundamental characteristic of such heterointerfaces is their morphology. Interface roughness causes inhomogeneous line-shape broadening, which usually dominates the low-temperature luminescence, and contributes appreciably to the room-temperature spontaneous emission of quantum wells.[2–4] This roughness can be reduced during epitaxy[4–8] by the interruption of growth at each heterointerface[4,9] or by reduced growth rates.[10] Adsorbed atoms diffuse across the surface during the growth interruption, until they are incorporated into a step edge, or are immobilized by the arrival of other atoms.[11] This mechanism can result in the creation of large islands, within which the quantum-well thickness appears almost constant to recombining excitons.[12] For liquid-phase epitaxy (LPE), growth occurs close to equilibrium and at low supersaturation. In combination with dislocated and patterned substrates,[13,14] this technique can produce smooth or regularly stepped surfaces.[15]

In this paper, we describe the growth of extremely narrow $GaAs/Al_xGa_{1-x}As$ quantum wells (QW's) by liquid-phase epitaxy. The resulting interfaces are characterized by high-resolution transmission electron microscopy (TEM), by line-shape analysis (LSA) of time-resolved photoluminescence (PL), and by cathodoluminescence imaging. We directly visualize that locally, the thickness variations and the interface morphology in LPE grown quantum-well samples are comparable to those reported by molecular-beam epitaxy (MBE) and metal-organic chemical-vapor deposition grown QW's.[12,16]

II. CRYSTAL GROWTH

The quantum wells were grown from a Ga solution in a slider boat. Hydrogen (purified by a Pd-diffusion cell) was passed continuously through the system. A three-zone furnace provided uniform temperature in its 260-mm-long central zone. The 210-mm graphite boat was positioned within this zone to minimize undesirable temperature gradients.

The epitaxial layers were grown on undoped, semi-insulating GaAs substrates with a misorientation less than 0.1° from exact (100). The substrate size was 13 mm × 14 mm. The substrate was degreased with acetone and trichlorethylen, followed by a HCl and a polishing etch in $H_2So_4(80\%):H_2O_2(70\%)=3:1$ for 30 s at 50 °C.

Two separate boxes of the slider boat, each containing solution for GaAs for $Al_xGa_{1-x}As$ growth were used. The solution were composed of Ga metal (99.9999% purity), and pure undoped GaAs and Al metal (99.9999% purity) for the GaAs and Al-Ga-As layers, respectively. The liquidus temperature was deduced from the phase diagrams of Hsieh[17] and Teramoto, Kazumura, and Yamanaka.[18]

The Ga and As solutions were baked at 800 °C for 3 h for purification and outgassing. Al metal was then added to one of the solutions, the substrate placed in the boat, and the system reheated. Equilibrium was reached by annealing at a few degrees above the liquidus temperature (which is nearly the same for both the GaAs and the Al-Ga-As solutions) and the system cooled to room temperature at the rate of 0.1 K/min.

A schematic cross section of a typical sample is shown in Fig. 1. The ≈400-nm-thick $Al_xGa_{1-x}As$ barrier layer ($x\approx0.4$) was grown directly on the substrate in approximately 180 s. The GaAs QW ($L_z\approx1-2$ nm) was then deposited on the Al-Ga-As surface in 1 s. Finally, a ≈200-nm-thick $Al_xGa_{1-x}As$ barrier layer ($x\approx0.4$) was grown on the GaAs layers. The growth temperature for all samples was 640 °C. A supersaturation of 2 K was used for growth solutions to achieve good nucleation and to inhibit etch-back of the substrate or of the previously grown layers. The system was cooled to room temperature in about 30 min by removing the furnace immediately after growth.

Approximately 30 samples, grown at various temperatures, cooling rate, supersaturations of the growth solutions, and growth rates were characterized as described below. We restrict our discussion here to a few typical samples. It should be emphasized that we obtained reproducible results concerning thickness and interface roughness of the QW's for samples grown under identical conditions.

III. RESULTS AND DISCUSSION

We have examined these LPE grown samples by a set of complementary techniques. The atomic configuration

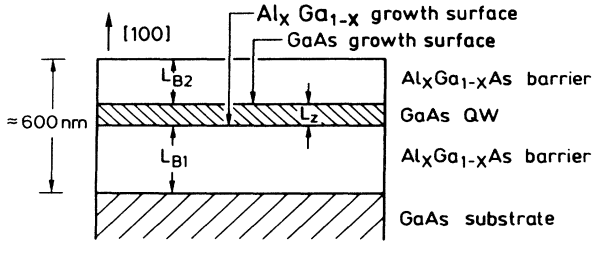

FIG. 1. Layer sequence of the QW samples.

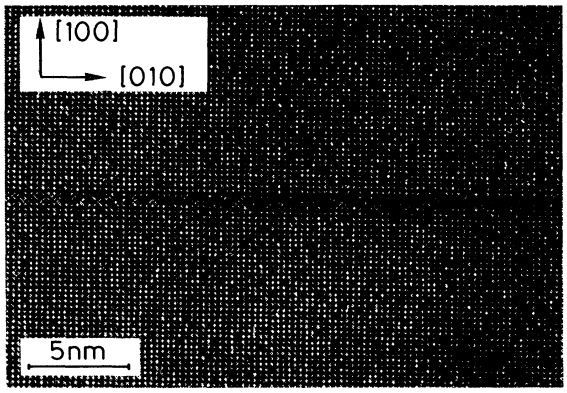

FIG. 2. High resolution TEM image of sample No. 1. The thickness of the GaAs QW, sandwiched between two $Al_xGa_{1-x}As$ layers ($x\approx0.4$), is about 3 ML. The spacing between the white dots is given by the spacing of atomic columns (2.8 Å) in $Al_xGa_{1-x}As$.

of the interfaces is deduced by chemical lattice imaging,[19] over fields of view of about 1000 Å. Luminescence techniques[12] were used to probe the interfacial configuration with excitons (diameter ~150 Å) over large fields of view (~100 μm).

A. High-resolution TEM

Figure 2 is a chemical lattice image[19] of sample No. 1, showing a small segment of the quantum well. The local thickness of the quantum well is ~3 monolayers (ML). However, the quantum-well thickness can vary significantly over the field of view depending on the actual position being inspected. Locally, the interfaces appear abrupt, although the interfacial roughness was not quantified by pattern recognition methods.[19] There is no evidence of significant intermixing or melt-back during LPE growth. Indeed, we believe the quantum well shown here to be the narrowest grown by LPE.

B. Photoluminescence and line-shape analysis

Photoluminescence was excited by the 476-nm line of a Kr^+-ion laser with an excitation density of 0.15 W/cm^2. The luminescence light was dispersed in a 0.5-m monochromator and detected by a photomultiplier. Figure 3 shows linear and semilogarithmic plots of the photoluminescence spectrum of sample No. 2 at 2 K. The luminescence of the $Al_xGa_{1-x}As$ barrier layers is also evident in the semilogarithmic plot. The Al content x, deduced from the energy position of 2.0552 eV of the bound exciton[20] is 42.8%.

A set of five emission lines (dotted line in Fig. 3), caused by excitonic $X(e,hh)_{n=1}$ recombination in the QW dominates the spectrum. The temperature and excitation intensity dependence of these lines prove their excitonic origin. Such splitting of the excitonic luminescence spectrum into distinct lines, observed in MBE

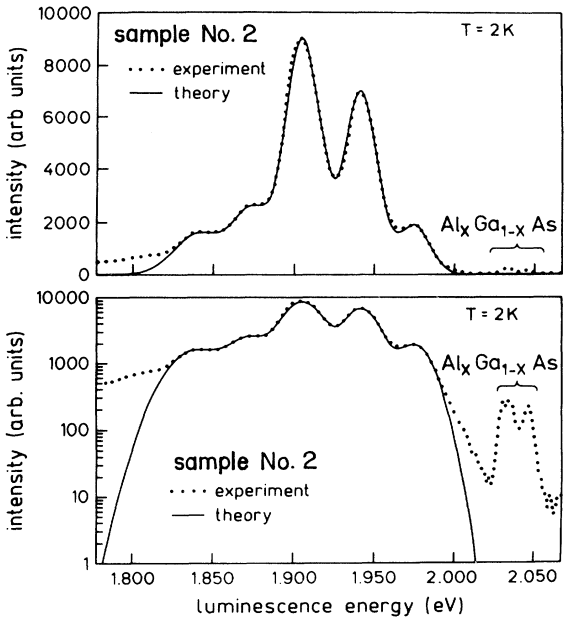

FIG. 3. Photoluminescence spectrum at 2 K of sample No. 2 in a linear and semilogarithmic display (solid lines) and in comparison to a theoretical fit (dotted).

QW's produced with growth interruption,[4,6,9,21] has not been previously reported for LPE QW's. The observation of a multiplet of spectral lines is a strong indication that radiative recombination of the excitons occurs within columns, within each of which the mean square root deviation of the quantum-well thickness, averaged over the exciton diameter by a large number of excitons, varies by much less than the difference between the different columns.

As shown by the solid line in Fig. 3, the observed spectral lines can be approximately fitted by a set of five simple Gaussians. This fit is further improved when the exponential energy dependence of the high-energy part of the luminescence, induced by the Maxwellian distribution of the excitons, is taken into account (see the logarithmic plot in Fig. 3). This line-shape model,[3,12,22] together with the effect of the exciton binding energy[23] can accurately reproduce the energies E_i of the subband edges. Using a finite square-well potential[24–26] the thickness L_z^i of the QW can be deduced from E_i. Additionally, the standard deviation of the energies σ_E^i, the standard deviation σ_{L_z} of the well width (i.e., the microscopic interface roughness), and the average island diameter d_i can all be calculated from these fits.[12,27]

The results of the LSA are listed in Table I. The width of the QW varies from ≈ 2.4 to 5.4 monolayers. (One monolayer equals 0.283 nm in the [100] direction.) The variation in thickness ΔL_z between adjacent columns is smaller than one monolayer ($\sim 0.7-0.8$ ML). The standard deviation of the energy σ_E increases from 10 to 15 meV with increasing well width. The corresponding standard deviation of the interface roughness σ_{L_z} ranges from 0.2 to 0.4 monolayers (Table I). Similarly, we deduce the diameter of the islands d_k to be $\approx 9-16$ nm. This is in close agreement with the local thickness variations observed in our chemical lattice images.

Similar experimental results have been obtained on many GaAs and $Al_xGa_{1-x}As$ LPE heterostructures.[28]

C. Time-resolved luminescence

For time-resolved measurements, the samples were excited by 5-ps laser pulses at an average power of 10 mW, with a repetition rate of 80 MHz. The emitted light was dispersed in a 0.32-m monochromator, and the entire spectrum detected by a two-dimensional Synchrosan streak camera with an S-1 cathode.

For sample No. 1, Fig. 4 shows a plot of the luminescence decay at $T=4$ K, as a function of luminescence photon energy. The excitation wavelength $\lambda_{exc}=615$ nm is slightly above the Al-Ga-As band gap. The luminescence of the $Al_xGa_{1-x}As$ barriers rapidly decreases, indicating the efficient carrier capture into the quantum well.[29]

The set of six excitonic luminescence lines, of lower energy than the Al-Ga-As luminescence, originates from columns in the GaAs QW as discussed above. None of the QW lines shows any peak wavelength shift with time. In particular, the relative intensities of the lines do not change with time. This absence of temporal variation in the relative intensities excludes significant carrier transfer between the different islands of the well. Thus, the mean extent of a column must be larger than the diffusion length of the carriers.[12] (The lack of carrier transfer between the islands was already suggested by the mutiplet

TABLE I. Results of the line-shape analysis of the luminescence spectrum of Fig. 3. E is the energetic position of the luminescence line, L_z is the calculated QW width, σ_E and σ_{L_z} are the standard deviations of the energy and of the well thickness, respectively, d_i is the island diameter.

E (eV)	L_z (nm)	$L_z(a/2)$	σ_E (meV)	$\sigma_{L_z}(a/2)$	d_i (nm)
1.9748	0.68	2.4	9.8	0.22	9
1.9420	0.88	3.1	10.0	0.21	14
1.9060	1.07	3.85	11.0	0.24	13
1.8735	1.30	4.6	11.5	0.27	11
1.8405	1.53	5.4	15.3	0.39	16

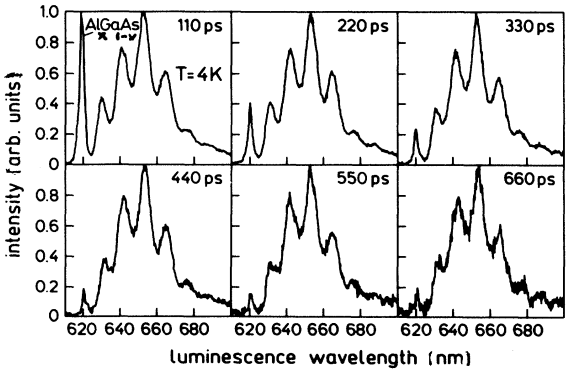

FIG. 4. Time-delayed luminescence spectra at $T=4$ K of sample No. 1. The fast decreasing $Al_xGa_{1-x}As$ line is distinguished from a set of six exciton lines $[X(e-hh)_{n=1}]$, originating from the columnar structure of the GaAs QW.

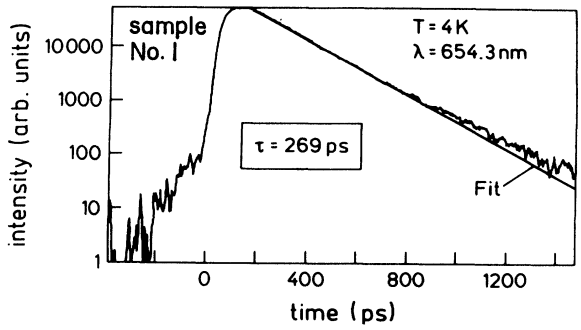

FIG. 5. The decay time of the luminescence line at $\lambda=654.3$ nm. The luminescence decay is exponential, as can be seen from comparison to the straight-line fit, in the semilogarithmic plot.

of lines in the low-temperature spectrum of Fig. 3, since the intensity of the higher-energy lines did not decrease with decreasing temperature. Such changes in intensity ratios were reported, e.g., in Ref. 12.)

Figure 5 shows the decay of the most intense line at a wavelength $\lambda=654.3$ nm. The decay is exponential over approximately three orders of magnitude. The deduced luminescence decay time is $\tau=270\pm10$ ps, which is closely similar to results obtained from MBE samples.[29,32] Our experiments do not reveal any significant variation of the excitonic lifetime in the different column within the QW's. This is also in agreement with time-delayed spectra, and is expected from theory for this range of well widths.[22] The average luminescence lifetime for all lines in Fig. 4 is also $\tau=270$ ps. Identical lifetimes were obtained for direct excitation of the well.

D. Cathodoluminescence imaging

Cathodoluminescence (CL) imaging of islands at heterointerfaces of quantum wells was first introduced by Bimberg *et al.*[12] We use a modified JEOL 840 scanning electron microscope as described in Ref. 33. The energy of the exciting electrons is 5 keV. Thus, the Bethe range

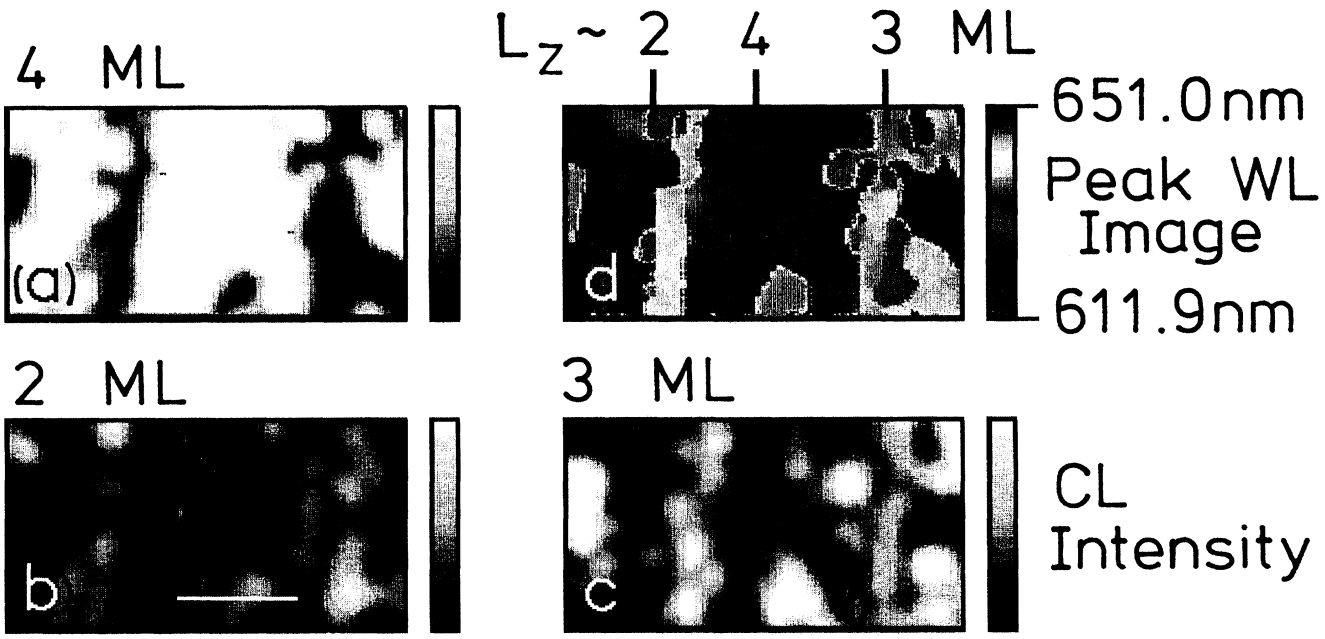

FIG. 6. Comparison of CL peak wavelength image (d) and simultaneously recorded CL intensity images for the 2- 3-, and 4-ML islands (a)–(c). Sample No. 2, temperature $T=9$ K. The features of the intensity images are complementary to each other and reproduce the characteristics of the wavelength image. The marker in (b) is 5 μm wide.

of the secondary electrons limits the lateral resolution of the present experiment to about 280 nm since the diffusion length is smaller. Measurements were performed at $T=5-9$ K. The luminescence light was dispersed in a 0.3-m McPherson vacuum monochromator, and the entire spectrum detected simultaneously by a reticon, covering a spectral range of 46.2 nm. An area of 128×100 pixels was scanned at the sample surface at varying magnifications, and a full spectrum taken at each of the 12 800 pixels.

Two experimental modes are available (see Refs. 27 and 33); in the peak-wavelength mode (CL wavelength imaging) only the wavelength of the most intense peak at each pixel is recorded. The data are presented either as a two-dimensional pseudocolor picture in which the wavelength is converted to a color, or as a three-dimensional plot. Thus, the micrometer-scale morphology of the various columns corresponding to the various peak wavelengths is revealed.

In the intensity mode (CL intensity imaging), for a chosen set of fixed wavelengths, the intensities are recorded within a given spectral range at each of the 128×100 pixels. Again, the intensity at each pixel can be converted into a color or a z coordinate. Thus, by selecting a particular luminescence line, the lateral distribution of a given quantum-well column is monitored.

Figure 6 shows a $T=9$ K CL wavelength image (d) and three CL intensity images (a)–(c) of sample No. 2. The photoluminescence spectrum of this sample is shown in Fig. 3. Figure 7 shows the three-dimensional representation of the wavelength image. The size of the area shown here is about $8\ \mu m\times16\ \mu m$. Three different luminescence lines dominate in various areas of Figs. 6(d) and 7. The lines at 626.8 nm (1.9137 eV), 637.6 nm (1.9440 eV), and 647.7 nm (1.9137 eV), approximately correspond to local thickness L_z of the QW column of 2, 3, and 4 ML, respectively. Since the thickness variations observed in the chemical images and the island sizes deduced from PL line-shape analysis are too small to be directly resolved by CL, the relatively abrupt micrometer-scale variations shown in Figs. 6 and 7 are most likely due to changes in the admixture of the different column heights over the sample, presenting changes of the mean quantum-well width on the order of an atomic layer. The extension of each such "column" ranges from 1 to 10 μm. This change of mean well width (columnar structure) in turn is caused by monatomic steps at the interfaces. The CL results thus directly probe the quantum-well morphology in the micrometer range, complementing the data obtained by chemical lattice imaging and PL measurements.

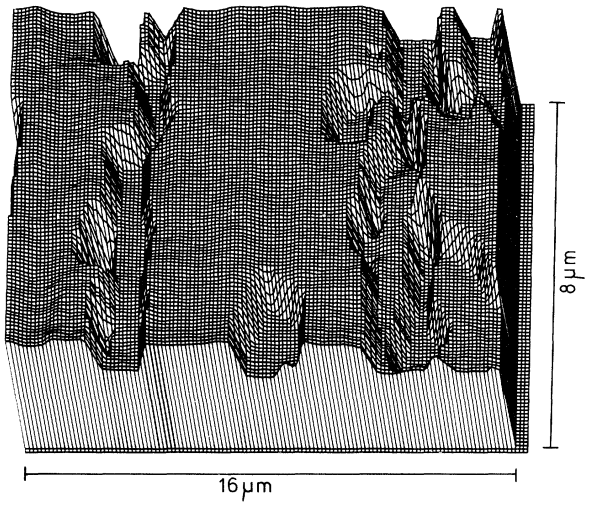

FIG. 7. CL wavelength image of sample No. 2 at 9 K, converted to a three-dimensional diagram. QW columns approximately 2, 3, and 4 ML thick are identified. The average island size is a few micrometers.

IV. CONCLUSION

In conclusion, we have shown that LPE can grow extremely narrow $GaAs/Al_xGa_{1-x}As$ quantum wells. Chemical lattice images have directly revealed the presence and microscopic nature of these QW's. Low-temperature photoluminescence yields distinct spectral lines originating from a columnar structure of the wells, within each of which the well thickness, as averaged over by many excitons, does not vary significantly. Line-shape analysis has been used to quantify the thickness ($L_z\approx2-6$ ML), an upper limit of the interface roughness ($\sigma_{L_z}\sim0.2-0.4$ ML), and the island diameter ($d_i\sim10$ nm). Time-resolved luminescence measurements reveal almost identical luminescence decay times $\tau\approx270$ ps for all observed luminescence lines. The cw and time-resolved results rule out significant carrier transfer between the columns. Consequently, the mean column size must be larger than the diffusion length of the carriers. Cathodoluminescence data directly image this micrometer-scale morphology of the quantum wells.

The interface morphology obtained here resembles closely the morphology found for GaAs QW's grown by MBE.[34] Köhrbrück *et al.* report interface roughness $t_L\approx0.2$ ML for 2-nm QW's and 0.2–0.3 ML for 5-nm QW's in addition to a columnar structure upon growth interruption at the GaAs surface of 100 s.

ACKNOWLEDGMENTS

We are very much indebted to R K. Bauer (Technische Universität Berlin) for supplying us with the photoluminescence spectra, to W. Rühle, H. Kalt, M. Alexander, and K. Rother (Max-Planck-Institut, Stuttgart) for time-resolved measurements, and to M. Krahl for a critical reading of the manuscript. Partial financial support by the "Stifterverband für die Deutsche Wissenschaft," and by "SFB 6" and "Str 277/1-1 of Deutsche Forschungsgemeinschaft" is gratefully acknowledged.

*Permanent address.

[1]See, e.g., the proceedings of the annual conference *Physics and Chemistry of Semiconductor Interfaces* (found in the July/August issues of J. Vac. Sci. Technol. B).

[2]C. Weisbuch, R. C. Miller, R. Dingle, A. C. Gossard, and W. Wiegmann, Solid State Commun. **37**, 219 (1982).

[3]J. Christen, M. Krahl, and D. Bimberg, Superlatt. Microstruct. **7**, 1 (1990); J. Christen and D. Bimberg, Phys. Rev. B **42**, 7213 (1990).

[4]D. Bimberg, D. Mars, J. N. Miller, R. Bauer, and D. Oertel, J. Vac. Sci. Technol. B **4**, 1014 (1986); J. Singh and K. K. Bajaj, Appl. Phys. Lett. **48**, 1077 (1986).

[5]C. W. Tu, R. C. Miller, B. A. Wilson, P. M. Petroff, T. D. Harris, R. F. Kopf, S. K. Sputz, and M. G. Lamont, J. Cryst. Growth **81**, 156 (1987).

[6]B. Deveaud, J. Y. Emergy, A. Chomette, B. Lambert, and M. Baudet, Appl. Phys. Lett. **45**, 1078 (1984).

[7]T. Y. Wang, K. L. Fry, A. Persson, E. H. Reihlen, and G. B. Stringfellow, Appl. Phys. Lett. **52**, 290 (1988).

[8]F. J. Stützler, S. Fujieda, M. Mizuta, and K. Ishida, Appl. Phys. Lett. **53**, 1923 (1988).

[9]M. Tanaka, H. Sakaki, J. Yoshino, and T. Furuta, Surf. Sci. **174**, 65 (1986).

[10]Ch. Maierhofer, S. Munnix, D. Bimberg, R. K. Bauer, D. E. Mars, and J. N. Miller, Appl. Phys. Lett. **55**, 1053 (1989).

[11]J. H. Neave, B. A. Joyce, P. J. Dobson, and N. Norton, Appl. Phys. A **31**, 13 (1983).

[12]D. Bimberg, J. Christen, T. Fukunaga, H. Nakashima, D. E. Mars, and J. N. Miller, J. Vac. Sci. Technol. B **5**, 1191 (1987).

[13]W. K. Burton, N. Cabrera, and F. C. Frank, Philos. Trans. R. Soc. London Ser. A **243**, 299 (1951); F. C. Frank, in *Crystal Growth and Characterization,* edited by R. Ueda, and J. B. Mullin (North-Holland, Amsterdam, 1975), p. 174.

[14]E. Bauser and H. Strunk, J. Cryst. Growth **69**, 561 (1984), and references therein.

[15]E. Bauser, in *Thin Film Growth Techniques for Low-Dimensional Structures,* edited by R. F. C. Farrow, S. S. P. Parkin, P. J. Dobson, J. H. Neave, and A. S. Arrott (Plenum, New York, 1987); U. Morlock, M. Kelsch, and E. Bauser, J. Cryst. Growth **87**, 343 (1988).

[16]S. Nilsson, A. Gustafsson, and L. Samuleson, Appl. Phys. Lett. **57**, 878 (1990); M. Grundmann, J. Christen, D. Bimberg, K. Streubel, and F. Scholz, Appl. Phys. Lett. (to be published).

[17]J. J. Hseih, in *Handbook on Semiconductors,* edited by Seymour P. Keller (North-Holland, Amsterdam, 1980), Vol 3, p. 415.

[18]I. Teramoto, M. Kazumura, and H. Yamanaka, Jpn. J. Appl. Phys. **18**, 1509 (1979),

[19]A. Ourmazd, J. Cunningham, D. W. Taylor, and J. A. Rentschler, Mater. Sci. Forum **38-41**, 689 (1989); A. Ourmazd, D. W. Taylor, and J. Cunningham, Phys. Rev. Lett. **62**, 933 (1989).

[20]D. J. Wolford, W. Y. Hsu, J. D. Daw, and B. G. Stratman, J. Lumin. **18/19**, 863 (1979).

[21]R. Köhrbrück, S. Munnix, D. Bimberg, D. E. Mars, and J. N. Miller, J. Vac. Sci. Technol. B **8**, 798 (1990).

[22]C. Colvard, D. Bimberg, K. Alavi, Ch. Maierhofer, and N. Nouri, Phys. Rev. B **39**, 3419 (1989).

[23]M. Grundmann and D. Bimberg, Phys. Rev. B **38**, 13 486 (1989); D. B. Tran Thoai, R. Zimmermann, M. Grundmann, and D. Bimberg, *ibid.* **42**, 5906 (1990).

[24]R. Dingle, in *Festkörperprobleme XV,* edited by H. J. Queisser (Vieweg, Braunschweig, 1975), p. 21.

[25]G. Bastard and J. A. Brum, IEEE J. Quantum Electron. **22**, 1625 (1986).

[26]M. Altarelli, J. Lumin. **30**, 472 (1985).

[27]J. Christen, in *Advances in Solid State Physics 30,* edited by U. Rössler (Vieweg, Braunschweig, 1990), p. 239.

[28]U. Morlock, Ph.D. thesis, Technische Universität Berlin (1989).

[29]J. Christen, D. Bimberg, A. Steckenborn, and G. Weimann, Appl. Phys. Lett. **44**, 84 (1984); Superlatt. Microstruct. **2**, 251 (1986); D. Bimberg, J. Christen, A. Steckenborn, G. Weimann, and W. Schlapp, J. Lumin. **30**, 562 (1985).

[30]B. Deveaud, T. C. Damen, J. Shah, and C. W. Tu, Appl. Phys. Lett. **51**, 828 (1987).

[31]M. Kohl, D. Heitmann, S. Tarucha, K. Leo, and K. Ploog, Phys. Rev. B **39**, 7736 (1989).

[32]J. Feldmann, G. Peter, E. O. Göbel, P. Dawson, K. Moore, C. Foxon, and R. J. Elliot, Phys. Rev. Lett. **59**, 2337 (1987).

[33]J. Christen, M. Grundmann, and D. Bimberg, Appl. Surf. Sci. **41/42**, 329 (1989).

[34]R. Köhrbrück, S. Munnix, D. Bimberg, D. E. Mars, and J. N. Miller, J. Vac. Sci. Technol. B **8**, 798 (1990); D. Bimberg, R. K. Bauer, D. Oertel, D. E. Mars, and J. N. Miller, J. Phys. **48**, C5-93 (1987).

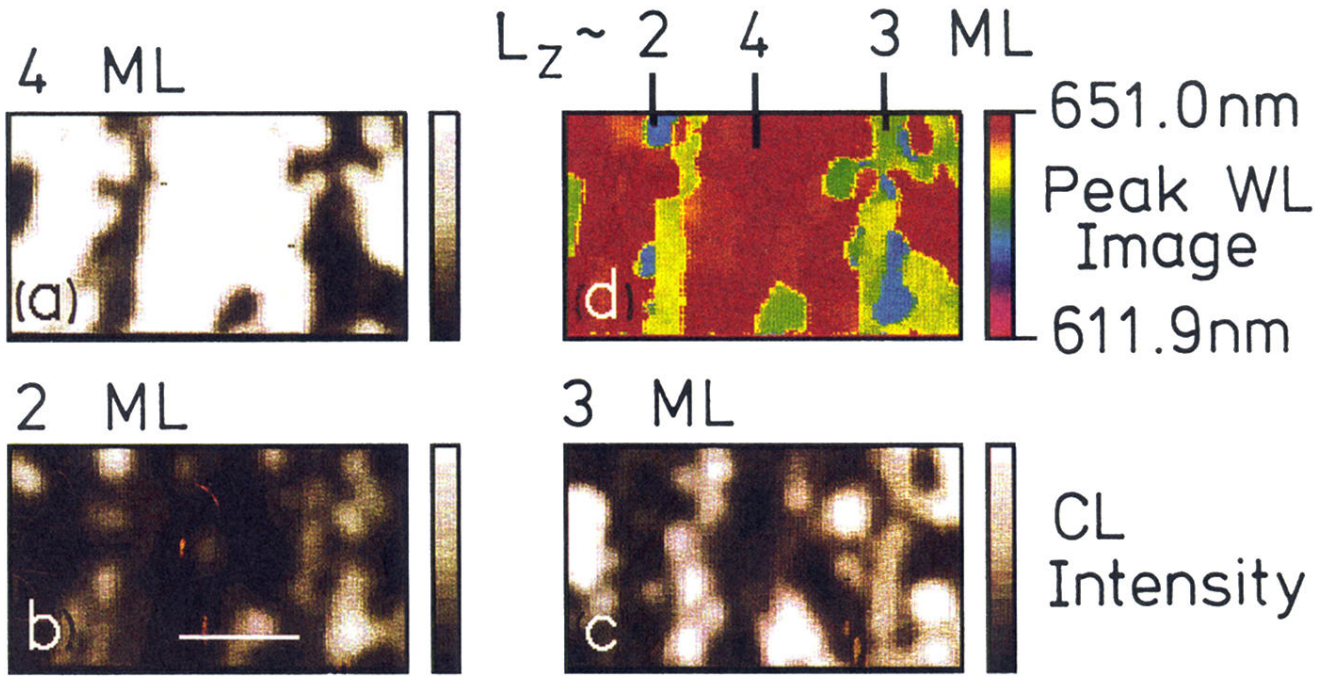

FIG. 6. Comparison of CL peak wavelength image (d) and simultaneously recorded CL intensity images for the 2- 3-, and 4-ML islands (a)–(c). Sample No. 2, temperature $T=9$ K. The features of the intensity images are complementary to each other and reproduce the characteristics of the wavelength image. The marker in (b) is 5 μm wide.